siRNA-mediated gene knockdown via electroporation in hydrozoan jellyfish embryos

[1] Tokiha Masuda-Ozawa, [2] Sosuke Fujita, [3] Ryotaro Nakamura, [3] Hiroshi Watanabe, [2] Erina Kuranaga, and [1,4] Yu-ichiro Nakajima*

1. Frontier Research Institute for Interdisciplinary Sciences, Tohoku University, Sendai, Japan
2. Graduate School of Life Sciences, Tohoku University, Sendai, Japan
3. Evolutionary Neurobiology Unit, Okinawa Institute of Science and Technology Graduate University, Okinawa, Japan
4. Graduate School of Pharmaceutical Sciences, The University of Tokyo

*Author for correspondence e-mail: nakaji97@g.ecc.u-tokyo.ac.jp
Tel: +81-3-5841-4863

Running title: **siRNA gene knockdown in jellyfish embryos**
Main text: 6487 words (Abstract: 258 words)
Figures: 5 **Supplementary information** (Figures: 7; Table: 5)
Keywords: siRNA, electroporation, cnidarian, hydrozoan, jellyfish, *Clytia, Cladonema*

Abstract

As the sister group to bilaterians, cnidarians stand in a unique phylogenetic position that provides insight into evolutionary aspects of animal development, physiology, and behavior. While cnidarians are classified into two types, sessile polyps and free-swimming medusae, most studies at the cellular and molecular levels have been conducted on representative polyp-type cnidarians and have focused on establishing techniques of genetic manipulation. Recently, gene knockdown by delivery of short hairpin RNAs into eggs via electroporation has been introduced in two polyp-type cnidarians, *Nematostella vectensis* and *Hydractinia symbiolongicarpus*, enabling systematic loss-of-function experiments. By contrast, current methods of genetic manipulation for most medusa-type cnidarians, or jellyfish, are quite limited, except for *Clytia hemisphaerica*, and reliable techniques are required to interrogate function of specific genes in different jellyfish species. Here, we present a method to knock down target genes by delivering small interfering RNA (siRNA) into fertilized eggs via electroporation, using the hydrozoan jellyfish, *Clytia hemisphaerica* and *Cladonema paciificum*. We show that siRNAs targeting endogenous *GFP1* and *Wnt3* in *Clytia* efficiently knock down gene expression and result in known planula phenotypes: loss of green fluorescence and defects in axial patterning, respectively. We also successfully knock down endogenous *Wnt3* in *Cladonema* by siRNA electroporation, which circumvents the technical difficulty of microinjecting small eggs. *Wnt3* knockdown in *Cladonema* causes gene expression changes in axial markers, suggesting a conserved Wnt/β-catenin-mediated pathway that controls axial polarity during embryogenesis. Our gene-targeting siRNA electroporation method is applicable to other animals, including and beyond jellyfish species, and will facilitate the investigation and understanding of myriad aspects of animal development.

Introduction

The phylum Cnidaria is the sister group to Bilateria, having separated from their common ancestor over 500 million years ago. Cnidarians have diversified their morphologies across an array forms, including corals, sea anemones, hydroids, and jellyfish, all of which are divided into two clades: Anthozoa and Medusozoa. The two differ in that Anthozoa includes only sessile polyp-type animals, while Medusozoa (Hydrozoa, Staurozoa, Scyphozoa, and Cubozoa) contains two forms: polyp and medusa, commonly known as jellyfish (Fig. 1A)[1,2]. The life cycle of most, though not all, jellyfish consists of five forms: gametes, fertilized eggs, planulae, polyps, and medusae[3]. Fertilized eggs undergo embryogenesis to become planula larvae, which metamorphose into sessile polyps. While vegetatively-growing polyps give rise to free-swimming medusae through the process of budding or strobilization, medusae sexually reproduce by releasing gametes. Due to their unique phylogenetic position, studies using cnidarians have provided evolutionary insight into development, regeneration, and behaviors in multicellular animals[1,4,5]. Despite divergent morphologies and lifestyles among cnidarians, to date, the molecular and cellular understanding of cnidarians has been acquired primarily using polyp-type animals such as the anthozoan *Nematostella vectensis* and the hydrozoan *Hydra* and *Hydractinia*. By contrast, jellyfish biology remains largely unestablished.

Among jellyfish species, the hydrozoan *Clytia hemisphaerica* is the best-studied laboratory model[6,7]. The well-established methodology for maintaining and propagating animals ensures a reliable source for daily experiments[8]. Transparent and small-sized medusae make whole-mount visualization achievable, and relatively large-sized eggs (~180 μm diameter) enable different manipulations via microinjection (Fig. 1B). Indeed, gene silencing by morpholino oligos and mRNA microinjection as well as gene knockout via CRISPR/Cas9 allow for the investigation of functions of genes of interest[9-13]. Furthermore, the *Clytia* genome assembly is complete, and transcriptome profiles are available for various stages and tissues, even at the single-cell level, which creates the foundation for research at the molecular level[12,14-18]. These resources and techniques, together with recently-established transgenesis[19], have accelerated research into numerous facets of distinct *Clytia* life stages. While initial studies focused on

95 embryogenesis, current research topics using *Clytia* include gametogenesis,
96 regeneration, and behavior exhibited by adult medusa [9,10,12,17,19,20].
97 Compared to the established model jellyfish *Clytia*, the hydrozoan *Cladonema*
98 *pacificum* is an emerging model that has recently been utilized for various studies in
99 development, regeneration, and physiology[21]. The ease of rearing all stages of
100 *Cladonema* without a filtration system or large water tank, along with their high
101 spawning rate, enable easy lab maintenance. Small-sized medusae with branched
102 tentacles allow for investigations of body size control and tentacle morphogenesis (Fig.
103 1C)[22-24]. *Cladonema* gametogenesis is regulated by a light-dark cycle as in *Clytia*, and
104 recent work has identified the neuropeptides involved in oocyte maturation[25].
105 Furthermore, *Cladonema* medusae possess eyes with a complex structure that includes
106 lenses (ocelli) in their tentacle bulbs, and studies using the closely related species
107 *Cladonema radiatum* have identified conserved light-sensitive opsins and regulators of
108 eye formation (*Pax*, *Six*, and *Eya*)[25-29], providing a model for the evolutionary
109 developmental biology of photoreceptor organs. Despite these attractive features of
110 *Cladonema* as a laboratory animal, no genome assembly or transcriptome is currently
111 available, and genetic manipulation techniques are only just being developed. One
112 major technical issue in manipulating *Cladonema* is their small eggs—with a diameter of
113 approximately 60 μm (Fig. 1C), regular microinjection is quite difficult. Establishing
114 genetic manipulations is required to facilitate the in-depth investigations needed to
115 further understand the biology of *Cladonema*, and an alternative method that eliminates
116 the need for microinjection would greatly facilitate that objective.
117 RNA interference (RNAi), the phenomenon of double stranded RNA (dsRNA)
118 mediated silencing of target genes, has been widely exploited in living organisms to
119 analyze gene function[30], primarily using chemically- or *in vitro*-synthesized double-
120 stranded small interfering RNAs (siRNAs) or vector-based short hairpin RNAs
121 (shRNAs)[31]. In cnidarians, siRNA-mediated gene silencing was initially applied to
122 *Nematostella* and *Hydra* polyps via soaking or electroporation[32-34]. More recently, gene
123 knockdown via shRNA microinjection or electroporation into eggs has been utilized in
124 studies with *Nematostella* and *Hydractinia* to show efficient reduction in gene
125 expression and associated phenotypes in early developmental stages[35-38]. In particular,
126 shRNA delivery via electroporation, which does not require the rigors of microinjection,

127 allows for the experimental gene knockdown of large numbers of individuals
128 simultaneously[36,38], opening up the possibility of manipulating genes in different aquatic
129 animals, even those that produce very small eggs like *Cladonema*.
130 The mechanism of RNAi-mediated gene repression after introducing foreign
131 dsRNA into cells involves the microRNA (miRNA) pathway, an endogenous gene
132 repression machinery conserved in both animals and plants[39]. In cnidarians, the
133 presence of the miRNA pathway has been demonstrated in *Nematostella* and
134 *Hydra*[32,40,41]. However, little is known about the endogenous RNAi pathway, especially
135 the presence and roles of miRNAs and the miRNA-related genes, in jellyfish such as
136 *Clytia* and *Cladonema*. Furthermore, in mammalian cultured cells, siRNAs can induce
137 gene repression independent of endogenous dsRNA processing factors, while shRNAs
138 cannot[42,43]. On this basis, we selected siRNA instead of shRNA for gene knockdown to
139 avoid the potential pitfall of dsRNA processing in jellyfish.
140 Here we report a gene knockdown method for jellyfish embryos with siRNA via
141 electroporation. Using two hydrozoan species, *Clytia hemisphaerica* and *Cladonema*
142 *pacificum*, we demonstrate that siRNA delivery into fertilized eggs effectively reduces
143 the expression of endogenous genes. We also confirm the known loss-of-function
144 phenotypes in *Clytia* after knocking down *GFP1* or *Wnt3*, which are induced in a dose-
145 dependent manner with siRNA. We further show that knockdown of *Wnt3* in *Cladonema*
146 embryos results in the reduction of gene expression of the oral marker *Brachyury* in
147 planula, implicating the Wnt/β-catenin pathway in the control of oral-aboral patterning.
148 Overall, our siRNA-mediated knockdown approach allows for the manipulation of a
149 large number of embryos through electroporation and enables functional analysis of
150 early development, providing a new experimental platform applicable to different jellyfish
151 species and other marine invertebrates.
152
153
154 ## Materials and Methods
155
156 **Animal culture and spawning induction**
157 *Clytia hemisphaerica* (Z11, Z4B as females and Z4C2, Z23 as males) and *Cladonema*
158 *pacificum* (6W as females and UN2 as males) were used for this research.

159 *Clytia hemisphaerica* were cultured using a previously reported method[8] with a
160 few modifications. Artificial sea water (ASW) was prepared using 220 g SEA LIFE
161 (Marin Tech) per 5L MilliQ water (Merk Millipore) with antibiotics (40 units/ml of penicillin
162 and 40 µg/ml of streptomycin). Medusae, embryos, and planula larvae were maintained
163 at 20ºC. Medusae were fed daily with Vietnamese brine shrimp (A&A Marine LLC, Elk
164 Rapids, MI, USA). Spawning timing was controlled by a 13 hours (h) dark /11 h light
165 cycle, and spawning was induced by light. Male and female medusae were transferred
166 into V-7 cups (AS ONE) before spawning (60 min for male and 90 min for female after
167 light stimulation).
168 *Cladonema pacificum* were cultured as previously described[23]. *Cladonema*
169 medusae were maintained at 22ºC in ASW, which was prepared using SEA LIFE (Marin
170 Tech) dissolved in tap water with chlorine neutralizer (Coroline off, GEX Co. ltd) (24
171 p.p.t) and antibiotics (40 units/ml penicillin and 40 µg/ml of streptomycin). Spawning
172 timing was controlled by a 30 min dark/23.5 h light cycle, and spawning of male and
173 female gametes was induced by dark stimulation. Before dark stimulation, adult females
174 and males were separately transferred into V7 cups (AS ONE) and 60 mm dishes (BD),
175 respectively.
176 *Nematostella vectensis* were cultured as previously described[44], with a few
177 modifications. Briefly, adult animals were maintained in brackish water at a salinity one-
178 third of artificial seawater (35 g/l, pH 7.5-8.0, SEA LIFE, Marin Tech) and fed with
179 freshly hatched artemia twice per week. Spawning induction was performed at 26°C
180 under light for at least 11 h.
181
182
183 **siRNA and shRNA**
184 siRNA sequences (19 mer RNA + 2 mer DNA) for *CheGFP1*, *CheWnt3*, and *CpWnt3*
185 were designed based on their CDS sequences by Nippon Gene Co., Ltd, and siRNA
186 duplexes were synthesized by manufacturers (Nippon Gene Co., Ltd and Sigma-
187 Aldrich, Merk). Lyophilized siRNA was resuspended in RNase free water to a final
188 concentration of 6 µg/µl as stock solution. The siRNA stock solution was diluted with
189 RNase free water to a total volume of 10 µl and then added to 90 µl of fertilized eggs in
190 15% Ficoll ASW just prior to electroporation.

191 shRNAs were synthesized as described in previous reports[36,38]. Briefly, shRNAs
192 were synthesized by *in vitro* transcription (IVT) from double stranded DNA templates
193 using the AmpliScribeTM T7-flashTM transcription kit (Lucigen, Inc.) and were purified
194 using Direct-Zol TM RNA Miniprep kits (Zymo Research, R2070). Concentrations of
195 shRNA was measured with a NanoDrop One (Thermo fisher).
196
197
198 **Collection of gametes and electroporation for *Clytia* and *Cladonema* fertilized**
199 **eggs**
200 For the preparation of gametes, sexually-mature *Clytia* medusae were treated following
201 a previously reported method[8], partially modified to fit our experimental equipment.
202 Adult male and female medusae were maintained on a 13 h dark/11 h light cycle, and
203 light stimuli induced gametogenesis in 60 min for sperm and 90 min for eggs (Fig. 2A).
204 For *Cladonema pacificum*, sexually-mature medusae were maintained on a 30 min
205 dark/23.5 h light cycle. Dark stimulation induced gametogenesis in 25 min for both
206 sexes.
207 Unfertilized *Clytia* and *Cladonema* eggs were collected and resuspended in 15%
208 Ficoll (Nacalai tesque, Japan) in ASW to prevent the eggs settling from at the bottom of
209 the microtube or sticking to the microtube surface, keeping the egg solution
210 homogeneous (Fig. 2B)[36,38]. Sperm water was added into the egg solution, and the
211 eggs and sperm were incubated for 5 min at room temperature (20-22ºC) until
212 fertilization occurred. The sperm water was then removed from the egg solution, and
213 fertilized eggs were resuspended in 15% Ficoll in ASW to adjust the total volume
214 needed for the number of electroporations. For each electroporation, 200-400 of *Clytia*
215 fertilized eggs or 200-700 of *Cladonema* fertilized eggs were prepared in 90 µl of 15%
216 Ficoll in ASW. 10 µl of siRNA/shRNA solution that was adjusted to the proper
217 concentration in RNase free water was added to the fertilized egg solution.
218 The total 100 µl of fertilized egg and RNA mixture was carefully transferred into a
219 4 mm cuvette using a 200 µl pipet tip and placed into the shockpod cuvette chamber
220 connected to the Gene Pulser Xcell (Bio-Rad). In most experiments, the Gene Pulser
221 Xcell was used for pulsing with a square wave voltage of 50 V and a single pulse
222 duration of 25 ms, except when optimizing electroporation conditions (Supplementary

223 Figs 1-2). After electroporation, fertilized eggs were transferred to a dish, and incubated
224 for 10 min. The 15% Ficoll solution was removed and replaced with new ASW, and the
225 samples were incubated at 20-22ºC.
226
227
228 **Collection of egg sacs, dejellying, and electroporation of *Nematostella* fertilized**
229 **eggs**
230 The collection of egg sacs, dejellying, and electroporation steps were performed as
231 previously described[36] with several modifications. Briefly, unfertilized egg sacs were
232 incubated in culture media with sperm at 20-25ºC for 30 min. The fertilized egg sacs
233 were then dejellied in freshly prepared L-Cysteine solution (0.04 g/ml, Nacalai tesque, in
234 brackish water; pH adjusted by 5N NaOH at 7.5-8.0) on a shaker for 10 min. The
235 dejellied eggs were rinsed with brackish water before they were suspended in Ficoll
236 solution (Sigma-Aldrich, in brackish water) at a final concentration of 15%. The
237 suspended eggs and siRNA (5 µg/µl stock solution, in MilliQ) were transferred to a 4
238 mm cuvette (Bio-Rad) with a final volume of 200 µl and were gently mixed. The Bio-Rad
239 Gene Pulser Xcell was used for pulsing, with a square wave voltage of 50 V and a pulse
240 duration of 25 ms. The samples were transferred to a 100 mm dish and maintained in
241 brackish water for 3 days.
242
243
244 **Imaging**
245 GFP and Rhodamine fluorescent imaging as well as bright field imaging, including *in*
246 *situ* hybridization imaging, were taken with an Axio Zoom V16 (ZEISS), and image
247 processing was done with ZEN 3.4 blue edition (ZEISS) and Fiji/ImageJ software[45].
248 Intensity of mean values of green fluorescence was measured using the average
249 brightness (pixel value) of the pixels. To prevent planula movement, we added 0.5 M
250 sodium azide (final concentration was less than 0.25M).
251
252
253 **Morphological quantification of planula larvae**

254 After *Wnt3* knockdown by siRNA electroporation of *Clytia* or *Cladonema*, we
255 approximated the planula body shape into a two dimensional ellipse, measured both the
256 long and short axes (Figs. 4C and 5D), and calculated the aspect ratio of those values
257 using Fiji/ImageJ software (Figs, 4D, 5E).
258
259
260 **RT-qPCR**
261 For *Clytia* and *Cladonema* samples, total RNA was extracted with RNeasy Mini or Micro
262 kits (Qiagen). Lysate was treated with DNaseI (Qiagen) for 15 min at room temperature
263 (RT). cDNA was synthesized with the PrimeScript II 1st strand synthesis kit (Takara bio).
264 RT-qPCR was performed with CFX connect (Bio-Rad) using iTaqTM universal SYBER
265 Green Supermix (Bio-Rad) or the QuantStudio 6 Flex Real-Time PCR System (Thermo
266 Fisher) using TB Green Premix Ex TaqII (Tli RNaseH Plus) (Takara, RR820). Gene
267 expression was normalized to the housekeeping gene, *EF1alpha* or *F-actin capping*
268 *protein subunit beta*, and the delta-delta-ct method was used for quantification (CFX
269 maestro software, Bio-Rad or QuantStudio 6 Flex Real-Time PCR System software,
270 Thermo Fisher).
271 For *Nematostella* samples, total RNA was extracted using the RNeasy Mini Kit
272 and RNase-Free DNase Set (Qiagen). cDNA synthesis was conducted using the
273 SuperScript IV First-Strand Synthesis System (Thermo Fisher). RT-qPCR was
274 performed with the StepOnePlusTM Real-Time PCR System (Applied Biosystems,
275 Thermo Fisher) using PowerUP SYBR Green Master Mix (Thermo Fisher). Gene
276 expression was normalized to the housekeeping gene, *NvEf1alpha,* and the delta-delta-
277 ct method was used for quantification (StepOne™ and StepOnePlus™ Software v2.3).
278
279
280 ***In situ* hybridization**
281 Purified total RNA was reverse transcribed into cDNA by PrimeScript™ 2 1st strand
282 cDNA Synthesis Kit (TaKaRa). The target gene fragments (*Brachyury*, *CpBra*) were
283 amplified from a cDNA library. The primer sets used for PCR cloning are as follows:
284 *CpBra*: 5'-GCTCCCATAAGATCCGGTCG -3'(forward) and 5'-
285 TTTGTCGCAGTCGAAGACCA-3'(reverse), or 5'-GAACGGTGATGGACAGGTCA-3'

286 (forward) and 5'-GGATTCCAAGGATTGGGCGT-3' (reverse). PCR products were sub-
287 cloned into the TAK101 vector (TOYOBO). The resulting plasmids were used for RNA
288 probe synthesis with digoxigenin (DIG) labeling mix (Roche), and T7 or T3 RNA
289 polymerase (Roche) was used, according to the insert direction. The detail for the probe
290 synthesis was referred to the published protocol[46].
291 Planula larvae were anesthetized in 50% 0.5 M NaN_3 in ASW for 5 min and fixed
292 overnight at 4°C with 4% paraformaldehyde (PFA) in ASW. The following whole mount
293 *in situ* hybridization was performed following the protocol in Hou et al.[24] with slight
294 modifications. Briefly, fixed samples were washed three times with PBS containing 0.1%
295 Tween-20 (PBST), followed by pre-hybridization in hybridization buffer (HB buffer:
296 5×SSC, 50% formamide, 0.1% Tween-20, 50 μg/ml tRNA, 50 μg/ml heparin) at 55°C for
297 2 h. Samples were hybridized with HB Buffer containing the antisense probes (final
298 probe concentration: 0.5-1 ng/μL in HB Buffer) at 55°C overnight. The samples were
299 washed each twice with wash buffer 1 (5x SSC, 50% formamide, 0.1% Tween-20),
300 wash buffer 2 (2x SSC, 50% formamide, 0.1% Tween-20) and 2x SSC. The samples
301 were then washed with 0.1% PBST and incubated in 1% blocking buffer (1% blocking
302 reagent [Roche, 11175041910] in Maleic acid) for 1 h. The samples were incubated with
303 alkaline phosphatase (AP)-conjugated anti-DIG antibodies (1:2000, Roche,
304 11175041910) in 1% blocking buffer for 4 h at room temperature. Colorimetric reactions
305 were performed by NBT/BCIP (Roche, 11175041910) in alkaline phosphatase buffer
306 (100 mM NaCl, 100 mM Tris-HCl (pH 9.5), 50 mM $MgCl_2$, 0.1% Tween-20) until the
307 signals were detected.
308
309
310 **Sequence alignment and phylogenetic analysis**
311 Amino acid sequence alignment of Wnt3 and Wnt family proteins were performed by
312 ClustalW[47]. GenBank accession numbers and protein names are listed in
313 Supplementary Table 3 and 4. The alignment data was visualized on Jalview software[48].
314 Maximum likelihood (ML) tree calculation was inferred on ClustalW with the PhyML
315 bootstrap method. Branch supports were computed out of 100 bootstrapped trees. The
316 tree visualization was created using MEGA-X software[49].
317

318

319 **qPCR primers**

Name	Sequence (5'->3')	
CpWnt3 qP FW	CAAATGTGGTCGATCAAACG	This study
CpWnt3 qP RV	TACGCCTTCTGCAACACTTG	This study
CpEF1-a_qPCR_F7	GGTCAATCTCGTTCCCTCCA	This study
CpEF1-a_qPCR_R7	TTTCCACCAGAGGTATCGGC	This study
CpBrachyury F	AAGGCGTATGTTTCCGGTCC	This study
CpBrachyury R	CAACGATGGTCTTCGACTGC	This study
CpFoxQ2a F	AGTTGGAGAAACAGCGTTCG	This study
CpFoxQ2a R	CCGTTCGCAAAGTCGTCAAA	This study
CpCapZbeta_qPCR_F	AAAGAAAGCTGGAGACGGTTCA	This study
CpCapZbeta_qPCR_R	GTAGTGGGCATTTCTTCCGC	This study
CheGFP1 qP F	TTGCTGTCCGAATAGTGCAG	Fourrage et al., 2014 Open Biol
CheGFP1 qP RV	GACAACTCCTCCTCCGAGTG	Fourrage et al., 2014 Open Biol
CheGFP1_2 qP F	ACAATCGCGTCACACTTAAAGG	This study
CheGFP1_2 qP RV	CGTTGTTTTCTTTGTCCGGC	This study
CheWnt3 qP F	ATCATGGCAGGTGGAAACTC	Leclère et al., 2012 Dev Biol
CheWnt3 qP RV	CCCCATTTCCAACCTTCTTC	Leclère et al., 2012 Dev Biol
CheEF1a qP F	TGCTGTTGTCCCAATCTCTG	Leclère et al., 2012 Dev Biol / Fourrage et al., 2014 Open biol
CheEF1a qP RV	AAGACGGAGTGGTTTGGATG	Leclère et al., 2012 Dev Biol / Fourrage et al., 2014 Open biol
NvEf1alpha FW	GGTTGCCTCTTCGCTTACCACT	This strudy
NvEf1alpha RV	CGTTCCTGGCTTTAGGACAC	This study
NvBra1_Fw_1032	CGGGCTCACACTCTCACTTA	This study
NvBra1_Rv1174	CTTGCGGTATGGTGTTCCAG	This study

320

321 **siRNA design**

Name	Sequence (5'->3')		ORF
siCheGFP1_1 sense	CCAUCAGCUUCGAAAAUGAdTdT	This study	HQ397706.1
antisense	UCAUUUUCGAAGCUGAUGGdTdT	This study	
siCheGFP1_2 sense	UGAUGGCGCUUAUAAAGUUdTdT	This study	HQ397706.1
antisense	AACUUUAUAAGCGCCAUCAdTdT	This study	
siCheGFP1_3 sense	CGGACUCAUUCUUCAAAAAdTdT	This study	HQ397706.1
antisense	UUUUUGAAGAAUGAGUCCGdTdT	This study	
siCheWnt3_1 sense	GCAUGUGACUGUAAAUUUAdTdT	This study	EU374721.1

antisense	UAAAUUUACAGUCACAUGCdTdT	This study	
siCheWnt3_2 sense	ACAGCUUGGUAAAAUGUUAdTdT	This study	EU374721.1
antisense	UAACAUUUUACCAAGCUGUdTdT	This study	
siCpWnt3_1 sense	GUGGAACUGUAGUGUUUCAdTdT	This study	EU374721.1
antisense	UGAAACACUACAGUUCCACdTdT	This study	
siCpWnt3_2 sense	AGCGUGUGCUGAAGGUAAAdTdT	This study	EU374721.1
antisense	UUUACCUUCAGCACACGCUdTdT	This study	
siNvBra1_1 sense	GAAGAGAUCACGAGUCUAAdTdT	This study	AF540387.2
antisense	UUAGACUCGUGAUCUCUUCdTdT	This study	
siNegative_Control-1 for Nv sense	GCAACACGCAGAGTCGTAAdT	Same sequence as Karabulut et al, 2019 Dev Biol	
antisense	TTACGACTCTGCGTGTTGCdT	Same sequence as Karabulut et al, 2019 Dev Biol	

shRNA template

Name	Sequence (5'->3')	
CheWnt3_SI1_F	TAATACGACTCACTATA GCATGTGACTGTAAATTTA TTCAAGAGA TAAATTTACAGTCACATGC TT	This study
CheWnt3_SI1_R	AAGCATGTGACTGTAAATTTATCTCTTGAATAAATTTAC AGTCACATGCTATAGTGAGTCGTATTA	This study
CheWnt3_SI2_F	TAATACGACTCACTATA ACAGCTTGGTAAAATGTTA TTCAAGAGA TAACATTTTACCAAGCTGT TT	This study
CheWnt3_SI2_R	AAACAGCTTGGTAAAATGTTATCTCTTGAATAACATTTT ACCAAGCTGTTATAGTGAGTCGTATTA	This study

Graphs and statistical analysis

All graphs were prepared in Excel. To assess phenotypes and RT-qPCR statistical significance, we used the percentage values and delta-delta-Ct values to perform two-tailed Student's t tests, except in Figure 5F, where a one-tailed Student's t test was used. For statistics related to fluorescence intensity mean value and aspect ratio, Kolmogorov–Smirnov normality tests were used. All statistical tests were performed at https://www.socscistatistics.com.

Results

338 **Optimization of electroporation conditions**

339 In both hydrozoan jellyfish *Clytia hemisphaerica* and *Cladonema pacificum*,
340 gametogenesis is regulated by light-dark transitions[6,50]. A previous report showed that
341 *Clytia* medusae release eggs within 110-120 min and sperm within 60-90 min upon light
342 illumination after 3-8 h of darkness[12]. *Cladonema pacificum*, which live along coastal
343 areas in Japan, exhibit two types of gametogenesis depending on habitat: the dark-light
344 transition (light stimulation type) and the light-dark transition (dark stimulation type),
345 respectively. Dark stimulation *Cladonema* medusae, which we used in this study,
346 release eggs or sperm within 30 min of dark stimulus after 20-24 h of constant exposure
347 to light[25,50]. By utilizing the characteristic gametogenesis of these jellyfish species, we
348 can control egg/sperm release to induce fertilization at any time of day. Indeed, we
349 routinely obtained *Clytia* sperm within 60 min and *Clytia* eggs within 90 min of light on a
350 13h dark/11h light cycle (Fig. 2A). Similarly, we collected gametes from *Cladonema*
351 within 25 min of dark stimulation on a 23.5h light/30 min dark cycle (Fig. 2A).

352 To determine optimal electroporation parameters, we first tested different
353 electroporation conditions and monitored the delivery efficiency of the red fluorescent
354 dye Rhodamine-Dextran into unfertilized *Clytia* and *Cladonema* eggs (Supplementary
355 Figs. 1-2). Given that the average molecular weight of siRNA (21-mer, ~13,300 Da) is
356 similar to the molecular size of Rhodamine-Dextran (10,000 Da), electroporation trials
357 with Rhodamine-Dextran can visually confirm that small molecules are incorporated into
358 jellyfish eggs, as previously shown in *Hydractinia* eggs[38]. The collected eggs were
359 suspended in 15% Ficoll artificial seawater to prevent precipitation and to make a
360 homogeneous solution (Fig. 2B)[36,38]. We performed electroporation trails for
361 Rhodamine-Dextran using a cuvette with a 4 mm gap and tested several conditions of
362 voltage (V) and pulse length time (milliseconds, ms) using a conventional
363 electroporation system (Fig. 2C). As previous work showed that increasing the number
364 of pulses does not increase the Dextran delivery rate but decreases the survival rate of
365 embryos[38], we fixed the number of pulses to one and incubated unfertilized eggs with 1
366 mg/ml Dextrane-Rhodamine solution. *Clytia* eggs have little autofluorescence in the red
367 channel, and without electroporation (No EP), red fluorescence was rarely detected in
368 unfertilized eggs (Fig. 2D and Supplementary Fig. 1A). We compared the eight different
369 electroporation conditions and found that the rhodamine fluorescence was detected in

370 *Clytia* eggs and correlated with the strength of electric voltage, as long as the voltage
371 was in the range of 50-100 V（Supplementary Figs. 1B-1D）. By contrast, when the
372 voltage exceeded 200 V, the eggs ruptured from physical damage, and cellular debris
373 was observed（Supplementary Figs, 1E-1G）.
374 We performed similar electroporation trials on unfertilized *Cladonema* eggs under
375 eight different conditions. While red autofluorescence was negligible in the *Cladonema*
376 eggs in the absence of electroporation (Fig. 2D and Supplementary Fig. 2A),
377 Rhodamine fluorescence was frequently detected with 50 V (Fig. 2D and
378 Supplementally Fig. 2E). In the more intense conditions beyond 100 V (Supplementally
379 Figs. 2F and 2G), the eggs were severely damaged. Based on these results, we
380 established the optimal electroporation conditions (50 V, 1 pulse, 25 ms) that provide
381 high frequency of Dextran-positive eggs and low levels of cell damage for both jellyfish
382 eggs (Fig. 2D). Of note, during the initial trials, we used unfertilized eggs, but we found
383 that the electroporation process severely affected the survival rate of subsequent
384 embryos. In the case of *Cladonema*, electroporation before fertilization severely
385 decreased the survival rate of fertilized eggs (7.04% at 1 h post fertilization) while
386 electroporation after fertilization did not influence the survival rate (No EP: 59.67%, With
387 EP: 60.15%) (Supplementary Table 1). This dissimilarity is likely due to the decrease of
388 fertilization rate after electroporation, and both elapsed time after spawning and physical
389 damage by electroporation can affect fertilization efficiency. Therefore, we decided to
390 conduct further electroporation experiments with fertilized eggs.
391
392
393 **Gene knockdown with siRNA in *Nematostella vectensis***
394 Before attempting gene knockdown via siRNAs electroporation in fertilized jellyfish
395 eggs, we first used *Nematostella vectensis,* where egg electroporation methodology has
396 been established[36]. We selected *Nematostella Brachyury* (*NvBra*), a gene expressed in
397 the blastopore margin that functions in the early embryo[51,52], as a target. After
398 electroporation of siRNA targeting *NvBra* in fertilized eggs, we examined *NvBra*
399 expression in planula larvae at 3 days-post-fertilization (dpf) by RT-qPCR and found
400 that *NvBra* expression was drastically suppressed compared to no electroporation
401 controls and negative control siRNAs (Supplementary Fig. 3). We further evaluated

402 survival rates after electroporation and confirmed that siRNA electroporation does not
403 severely affect survival rates of 3 dpf planula in any of the tested conditions
404 (Supplementary Table 2). These results suggest that siRNA delivery into fertilized eggs
405 via electroporation is an effective gene knockdown method that is comparable to the
406 effect of shRNA delivery into unfertilized eggs via electroporation[36], supporting our
407 attempt to perform gene knockdown via siRNA electroporation using fertilized jellyfish
408 eggs.
409
410
411 **Endogenous *GFP1* knockdown with siRNA in *Clytia hemisphaerica***
412 The hydrozoan jellyfish *Clytia* endogenously expresses green fluorescent proteins,
413 which are encoded by 14 genes grouped into 4 clusters (*CheGFP1-4*)[16]. The expression
414 pattern for each GFP changes by stage in the life cycle: for instance, *Clytia* eggs
415 express maternal *CheGFP2* mRNA, and planula larvae show typical ring-like *CheGFP1*
416 fluorescence in the lateral ectoderm at 3 dpf[11]. While *CheGFP1* gene expression
417 becomes dominant in the planula stage; *CheGFP2, CheGFP3,* and *CheGFP4* are
418 expressed in different tissues and organs in the medusa[53]. Momose *et al*. succeeded in
419 genome editing by injecting CRISPR/Cas9 targeting the endogenous *CheGFP1* into
420 fertilized eggs, and confirmed the knockout effect by loss of green fluorescence in 3 dpf
421 planula larvae[11]. In addition, *CheGFP1* is not essential for animal survival, which allows
422 for the monitoring of knockdown effects after embryogenesis. For these reasons, we
423 chose endogenous *CheGFP1* for the first target gene of siRNA knockdown.
424 In order to maximize the effect of gene knockdown, we used a combination of
425 three different siRNAs against *CheGFP1* (Accession No. HQ397706.1; Supplementary
426 Fig. 4A) in a mixture with a 1:1:1 ratio, and electroporated 600 ng/μl of siRNA mix (200
427 ng/μl per each siRNA) into fertilized eggs (Fig. 3A). To verify the effect of gene
428 knockdown, we measured green fluorescence intensity in 2 dpf planula and found that
429 siRNA (600ng/μl siRNA mix) electroporated embryos showed dramatically reduced
430 fluorescence intensity compared to the no-siRNA controls (Figs. 3B-D; mean intensity
431 value: 5.7×10^3 for 0 ng/μl control, 1.8×10^3 for 600 ng/μl). To evaluate the knockdown
432 effects at varying doses of siRNA, we next electroporated different concentrations of the
433 *CheGFP1* siRNA mix (0, 150, 300, and 600 ng/μl) into fertilized eggs. While control 3

434 dpf planulae with no-electroporation (No EP) as well as those with no-siRNA showed
435 typical ring-shape GFP fluorescence in the ectoderm, many planulae with *CheGFP1*
436 siRNA electroporation lost green fluorescence（Figs. 3E-3H）. To evaluate the GFP
437 knockdown effects, we classified planulae with typical GFP1 fluorescence as “wild type”
438 and planulae with reduced fluorescence as “reduced” for further quantification (Figs. 3I
439 and 3J). The percentage of wild type phenotype dramatically reduced in an siRNA dose-
440 dependent manner (Fig. 3K). To further quantify the above result on a molecular level,
441 we examined relative *CheGFP1* mRNA levels by RT-qPCR using the primer set that
442 was evaluated in a previously study[53]. Consistent with the image analysis results, we
443 confirmed a marked reduction of *CheGFP1* gene expression at different concentrations
444 of *CheGFP1* siRNA (Fig. 3L). These results demonstrate that siRNAs targeting
445 *CheGFP1* repress its expression upon electroporation and that the knockdown effects
446 are dose-dependent.
447 Given the presence of multiple *CheGFP1* loci (seven nearly identical *CheGFP1*
448 genes) in the *Clytia* genome[16], it was not clear whether three siRNAs against *GFP1*
449 sufficiently suppress gene expression in different versions of *CheGFP1*, particularly
450 those expressed in the planula stage (Supplementary Fig. 4A）. We thus performed RT-
451 qPCR using the newly designed primer set that amplifies all seven *CheGFP1* genes and
452 found a dramatic reduction of gene expression upon electroporation of *CheGFP1*
453 siRNAs (600 ng/μl)（Supplementary Fig. 4B）. Altogether, these results indicate that our
454 combination of *CheGFP1* siRNAs suppresses gene expression of *CheGFP1* in the
455 *Clytia* planula.
456
457
458 ***Wnt3* knockdown with siRNA in *Clytia hemisphaerica***
459 Since electroporation of siRNAs targeting endogenous *CheGFP1* was shown to be
460 effective, we next decided to investigate the effects of knocking down other genes that
461 play important roles in early development. Wnt3 is a secreted signaling protein in the
462 Wnt/β-catenin pathway that is involved in diverse developmental processes including
463 cell fate decisions and patterning[54,55]. In *Clytia*, *Wnt3* RNA is maternally localized to the
464 animal cortex, the future oral side of the embryo, and Wnt3 organizes axial patterning
465 as the main ligand for the Wnt/β-catenin pathway in the early embryonic stage[10]. After

466 embryogenesis, the *Clytia* planula normally elongates along the oral-aboral axis and
467 becomes oval in shape（Fig. 4A）. By contrast, after *CheWnt3* morpholino injection, the
468 morphant loses oral-aboral axis polarity and exhibits a spherical shape[10]. This raises the
469 possibility that knockdown of *CheWnt3* via siRNA may result in a similar spherical
470 morphology for *Clytia* larvae as is observed in *CheWnt3* morphants. Therefore, to
471 evaluate siRNA knockdown effects on *Clytia*, we chose *CheWnt3* as our second target.
472 We used a mixture of two different siRNAs (1:1 ratio) targeting *CheWnt3*, and
473 carried out electroporation of the siRNA mix into *Clytia* fertilized eggs. After
474 electroporation of *CheWnt3* siRNAs, 1 dpf planula larvae showed nearly complete
475 spherical morphology (Fig. 4B), which is reminiscent of *CheWnt3* morphants[10]. To
476 quantify the effect of siRNA knockdown on *Clytia* larval morphology, we calculated the
477 aspect ratio in two dimensions, where values greater than 1.0 shows the tendency to be
478 oval (ellipsoid-like) while a value of 1.0 indicates a perfect circle (sphere) (Fig. 4C). The
479 control larvae with 0 ng/μl siRNA showed a median aspect ratio of 1.69, indicating a
480 typical ellipsoid-like morphology. By contrast, larvae that underwent electroporation with
481 *CheWnt3* siRNAs (400 ng/μl) showed a median aspect ratio of 1.16, suggesting a much
482 greater tendency toward spherical morphology (Fig. 4D). These results quantitively
483 confirmed the effect of *CheWnt*3 knockdown on larval morphology, which phenocopies
484 *CheWnt3* morphants[10]. To analyze the level of gene-specific knockdown at varying
485 doses of siRNAs, we next electroporated mixtures of 0, 100, 200, and 400 ng/μl of
486 *CheWnt3* siRNAs into *Clytia* fertilized eggs (Figs. 4E-4H). To evaluate *CheWnt3* siRNA
487 effects on morphology, we classified 1 dpf planulae with elongated ellipsoid-like shapes
488 as “normal” and planulae with spherical shapes as “spherical” (Figs. 4I and 4J). The
489 percentage of normal phenotype dramatically reduced after *CheWnt3* siRNA-
490 electroporation (< 1.0 % in 400 ng/μl), even at the lowest dose (5.2% in 100 ng/μl) (Fig.
491 4K). To further evaluate the result at a molecular level, we analyzed relative *CheWnt3*
492 mRNA levels by RT-qPCR and confirmed a significant reduction in *CheWnt3* gene
493 expression at all concentrations (Fig. 4L). Of note, after electroporation with universal
494 negative control siRNA（Nippon Gene Co., Ltd.）, both morphological phenotypes and
495 relative gene expression were comparable to no-siRNA controls (Figs. 4K and 4L),
496 further confirming that siRNA-mediated knockdown by electroporation is target-specific.

497 These results together indicate that siRNAs targeting endogenous genes effectively
498 knock down their expression in *Clytia* embryos.
499 Effective gene knockdown via shRNA electroporation has previously been
500 reported using two cnidarian polyps, *Nematostella vectensis* and *Hydractinia*
501 *symbiolongicarpus*[36,38]. To test whether shRNAs are also effective in the hydrozoan
502 jellyfish *Clytia*, we designed shRNAs targeting *CheWnt3* using the same 19 bp target
503 sequence that was used for siRNAs, and performed electroporation on fertilized eggs
504 with a mix of two different *Wnt3* shRNAs. After electroporation of *Wnt3* shRNAs, relative
505 *Wnt3* mRNA expression in 1 dpf planula was weakly down-regulated (0.83), and was
506 not significant compared to the striking effects of *Wnt3* siRNA electroporation (0.039) at
507 the same concentration (400 ng/μl) (Fig. 4L). In addition, electroporation of *Wnt3*
508 siRNAs resulted in an extensive morphological change toward spherical shaped
509 planulae, showing almost no "normal" phenotype (0.71%), whereas electroporation of
510 shRNA had a limited effect (60.4%) (Fig. 4K). These results suggest that the effect of
511 siRNA is much stronger than that of shRNA in *Clytia* when treated with the same target
512 sequence and concentration.
513
514 **Identification of *Wnt3* in *Cladonema pacificum***
515 In contrast to *Clytia*, the sole genetic model jellyfish, previous studies have neither
516 established genetic manipulation nor performed genome sequencing of *Cladonema*
517 *pacificum*, despite its unique biological features. This is partly because the extremely
518 small size of the *Cladonema* egg makes microinjection difficult. By testing whether
519 siRNA-mediated knockdown via electroporation can work in *Cladonema*, we can start to
520 manipulate genes in *Cladonema* while also demonstrating that siRNA electroporation
521 can be applicable to other jellyfish species. While green fluorescent protein (GFP) is
522 often an easy early target for gene manipulation in emerging organisms, *Cladonema*
523 does not exhibit apparent endogenous green fluorescence expression at any stage,
524 unlike *Clytia*. We instead turned our focus to *Wnt3* as the target for gene knockdown in
525 *Cladonema* since Wnt3 plays an important role in early embryonic development in
526 several cnidarian species[56,57].
527 To identify the *Wnt3* ortholog in *Cladonema*, we utilized RNA-seq results from the
528 *Cladonema* polyp, stolon, and medusa manubrium (data not shown). We performed

529 *Cladonema Wnt3* CDS annotation using the *Clytia* CDS database (MARIMBA, Marine
530 models database: http://marimba.obs-vlfr.fr) and found one contig annotated with *Wnt3*
531 (*CpWnt3*) and multiple *Wnt* genes (Supplementary Figs. 5 and 6). We then performed
532 phylogenic analysis using the neighbor-joining method, and confirmed *CpWnt3*
533 (LC720435) is grouped with medusozoan *Hydra vulgaris* (*HvWnt3*) and *Clytia Wnt3*
534 (*CheWnt3*) rather than Anthozoa *Nematostella* and *Acropora digitifera* (Supplementary
535 Fig. 5A). Multiple sequence alignment further showed highly conserved amino acids
536 sequences among different species including bilaterians and cnidarians (Supplementary
537 Fig. 5B). These findings raise the possibility that *CpWnt3* has a similar function in
538 controlling the Wnt/β-catenin pathway in *Cladonema.*
539
540
541 ***Wnt3* knockdown with siRNA in *Cladonema pacificum***
542 Does *Wnt3* function during *Cladonema* embryogenesis, particularly during axial
543 patterning? Interestingly, *Cladonema* planula larvae do not show a clear elongated
544 shape (Fig. 5A), as observed in *Clytia*. It is thus possible that morphogenesis, including
545 axial patterning and/or Wnt/β-catenin pathway function, differs between these two
546 jellyfish species. It is also possible that the limited elongation in *Cladonema* planulae
547 might hamper phenotypical appearance upon inhibition of Wnt/β-catenin signaling.
548 In order to verify that siRNA electroporation works in *Cladonema* and that *Wnt3*
549 affects axial patterning, we performed electroporation of siRNAs targeting *CpWnt3*. We
550 prepared fertilized *Cladonema* eggs as we did in *Clytia*, and used a mixture of two
551 different siRNAs against *CpWnt3* CDS with a 1:1 ratio (300 ng/μl) and performed
552 electroporation with the previously established parameters (50V, 1 pulse, 25 ms) in
553 fertilized *Cladonema* eggs. After electroporation of siRNAs for *CpWnt3*, planula larvae
554 did not exhibit morphological differences compared to controls（Figs. 5A-5C; median
555 aspect ratio: 1.21 for 0 ng/μl control, 1.16 for 300 ng/μl for si*CpWnt3*）. We then
556 quantified the morphological phenotypes by calculating the aspect ratio of 1 dpf
557 planulae and confirmed that *CpWnt3* knockdown does not cause a significant
558 morphological change (Figs. 5D and 5E), which is consistent with the possibility that
559 *Cladonema* planulae simply exhibit limited elongation.

560 Another possibility that would explain the above result is a defect in the siRNA
561 knockdown itself. To test this potential explanation, we carried out RT-qPCR using
562 mRNA samples from 1 dpf planula after electroporating different concentrations of
563 *CpWnt3* siRNA mix (0, 150, and 300 ng/μl) into fertilized eggs. We confirmed a
564 reduction of *Wnt3* gene expression in an siRNA dose-dependent manner (Fig. 5F),
565 eliminating siRNA knockdown defects as the cause of our initial result.
566 To further confirm whether the Wnt/β-catenin pathway is affected by *Wnt3*
567 knockdown, we examined the gene expression of axial markers *Brachyury* (*CpBra*) and
568 *FoxQ2a* (*CpFoxQ2a*), whose expression are influenced by the Wnt/β-catenin pathway in
569 *Clytia*[10]. From RT-qPCR, we found that *CpWnt3* knockdown causes a decrease in
570 *CpBra* gene expression and an increase in *CpFoxQ2a* gene expression (Supplementary
571 Fig. 7). We also examined *CpBra* expression by *in situ* hybridization and confirmed the
572 reduction of *CpBra* expression on the oral side of planula larvae (Figs. 5G-5I), which is
573 similar to the phenotype exhibited by *CheWnt3* morphants in *Clytia*[10]. Notably, after
574 *CpWnt3* siRNAs electroporation, the rate of metamorphosis from planula to primary
575 polyp decreased dramatically (Supplementary Table 5), implying potential
576 developmental defects upon abrogation of the Wnt/β-catenin pathway. These results
577 suggest that, although overall oral-aboral polarity is less prominent in *Cladonema*
578 compared to *Clytia* at the morphological level, the axial patterning mechanism mediated
579 by Wnt/β-catenin signaling may be conserved between these two jellyfish species.
580
581

582 **Discussion**

583 In this study, we have established a method to knock down endogenous genes in two
584 hydrozoan jellyfish, *Clytia hemisphaerica* and *Cladonema pacificum*, via the siRNA
585 electroporation of fertilized eggs. We showed that knockdown of endogenous *GFP1* in
586 *Clytia* causes the loss of GFP fluorescence in the planula stage (Fig. 3), as previously
587 achieved by CRISPR/Cas9-mediated *GFP1* knockout[11]. We also confirmed that
588 knockdown of *Wnt3* in *Clytia* induces spherical morphology of the planula (Fig. 4),
589 mirroring the results of injections of *Wnt3* morpholino antisense oligo[10]. We further
590 succeeded in efficient repression of *Wnt3* gene expression in *Cladonema* after *Wnt3*
591 siRNA electroporation and found that expression of axial patterning genes is controlled

592 by the Wnt/β-catenin pathway (Fig. 5), suggesting that the conserved mechanism is
593 involved in embryogenesis and planula morphogenesis across hydrozoan jellyfish
594 species.
595 Our results show that the knockdown efficiency of siRNA is much greater than
596 that of shRNA for electroporation of *Clytia* fertilized eggs with the same *Wnt3* target
597 sequence in the same concentration (Fig. 4K-4L). One possibility that would explain
598 such distinct effects between siRNA and shRNA electroporation is the existence of
599 differences in the RNAi machinery or RNA processing efficiency among cnidarians.
600 During RNAi in mammals, the RNase III Dicer protein processes shRNA in collaboration
601 with cofactors TRBP (Transactivation response element RNA-binding protein) and
602 PACT（protein activator of the interferon-induced protein kinase）to produce a mature
603 form of siRNA[39]. Mature siRNA in the Dicer and TRBP/PACT complex is associated
604 with the Argonaute protein and cleaves endogenous complementary mRNAs as the
605 RNA-induced silencing complex [30,58]. These small RNA biogenesis factors, Dicers and
606 cofactors (TRBP in bilaterians, HYL1 in plants and cnidarians), are found in
607 *Nematostella vectensis, Acropora digitifera,* and *Hydra vulgaris*[41]. Although Dicers
608 (TCONS_00004571 and TCONS_00004525) and Hyl1 (TCONS_00010722) are
609 predicted to exist in *Clytia* based on MARIMBA transcriptome data, the expression level
610 of Dicers in oocytes and early gastrulation stages is lower than that in other stages,
611 suggesting the possibility that insufficient shRNA to siRNA processing efficiency is
612 responsible for the difference in knockdown efficiency between siRNA and shRNA
613 electroporation. It will be interesting to elucidate the detailed molecular mechanism of
614 RNAi in different cnidarian species and address RNA processing efficiency in distinct
615 developmental stages. The lower efficiency of knockdown by shRNA compared to
616 siRNA in *Clytia* could also be simply explained by lower shRNA electroporation
617 efficiency. This possibility could be tested by inserting shRNA or siRNA into fertilized
618 eggs by microinjection, instead of electroporation, which would be followed by
619 assessing gene expression and phenotypes.
620 During *Clytia* early embryogenesis, *Wnt3* RNA is localized to the animal cortex of
621 the egg and contributes to the formation of the oral-aboral axis[10]. Accordingly,
622 knockdown of *Wnt3* in *Clytia* fertilized eggs induces suppression of axis formation and
623 planula elongation (Fig. 4). In contrast, despite the fact that no morphological phenotype

624 was observed after *Wnt3* knockdown in *Cladonema*, gene expression of the conserved
625 axial patterning genes, *Brachyury* and *FoxQ2a,* was disrupted (Figs. 5G-5H and
626 Supplementary Fig. 7). In addition to *Clytia,* the Wnt/β-catenin pathway is involved in
627 axis formation during cnidarian embryogenesis including *Nematostella*[44,56,59]*,*
628 *Acropora*[60]*, and Hydractinia*[57]. Furthermore, given that the Wnt/β-catenin pathway is
629 also associated with axis formation during metamorphosis in *Hydractinia*[57,61] and
630 *Clytia*[62], the reduced metamorphosis rate observed in *CpWnt3* knockdown *Cladonema*
631 may be attributed to disrupted axis formation (Supplementary Table 5). Taken together,
632 our data support the pivotal role of Wnt/β-catenin signaling in cnidarian development.
633 An interesting feature of jellyfish is that their morphology dramatically changes
634 across their life cycle from planula to polyp and then to medusa. In particular, polyps
635 and medusae, different adult stages of the same animal, exhibit distinct regenerative
636 ability, lifespan, and behaviors. Although regeneration mechanisms have been
637 extensively studied in polyp-only animals such as *Hydra* and *Hydractinia*, classical
638 studies have used the medusa stage of several jellyfish species and demonstrated their
639 regenerative potential[21]. Recent work using *Clytia* medusae has further shown a
640 remarkable remodeling and repatterning mechanism orchestrated by muscle systems
641 upon organ loss[17]. At the behavior level, the medusae of the upside-down
642 jellyfish *Cassiopea* exhibit a sleep-like state[63], which is similarly observed in *Hydra*
643 polyps[64]. More recent work using transgenic *Clytia* has characterized feeding behaviors
644 in medusae at a neural-network resolution[19]. To understand how these diverse
645 biological processes in jellyfish are regulated at the molecular level, the functions of
646 specific genes at various stages must be analyzed. Although gene knockdown by
647 dsRNA electroporation into polyps in the scyphozoan jellyfish *Aurelia* has been
648 reported[65], gene knockdown at the medusa stage has not yet been achieved. Given that
649 siRNA electroporation is applicable to *Hydra* polyps[33,66] in addition to cnidarian fertilized
650 eggs, we now have a better chance to apply this technique to the medusa stage,
651 although, because they are susceptible to electric shock, electroporation parameters
652 must be optimized in order to achieve gene knockdown in medusae. Collectively, our
653 gene knockdown via siRNA electroporation method will complement the existing shRNA
654 electroporation approach in cnidarian polyps and will enable molecular-level analysis of
655 the vast biological phenomena exhibited across the different life stages in jellyfish.

656

657

658 ## References

659 1 Technau, U. & Steele, R. E. Evolutionary crossroads in developmental biology:
660 Cnidaria. *Development* **138**, 1447-1458, doi:10.1242/dev.048959 (2011).
661 2 Zapata, F. *et al.* Phylogenomic Analyses Support Traditional Relationships within
662 Cnidaria. *PLoS One* **10**, e0139068, doi:10.1371/journal.pone.0139068 (2015).
663 3 Leclere, L. & Rottinger, E. Diversity of Cnidarian Muscles: Function, Anatomy,
664 Development and Regeneration. *Front Cell Dev Biol* **4**, 157,
665 doi:10.3389/fcell.2016.00157 (2016).
666 4 Holstein, T. W., Hobmayer, E. & Technau, U. Cnidarians: an evolutionarily
667 conserved model system for regeneration? *Dev Dyn* **226**, 257-267,
668 doi:10.1002/dvdy.10227 (2003).
669 5 Bosch, T. C. G. *et al.* Back to the Basics: Cnidarians Start to Fire. *Trends*
670 *Neurosci* **40**, 92-105, doi:10.1016/j.tins.2016.11.005 (2017).
671 6 Houliston, E., Momose, T. & Manuel, M. Clytia hemisphaerica: a jellyfish cousin
672 joins the laboratory. *Trends Genet* **26**, 159-167, doi:10.1016/j.tig.2010.01.008
673 (2010).
674 7 Houliston, E., Leclere, L., Munro, C., Copley, R. R. & Momose, T. Past, present
675 and future of Clytia hemisphaerica as a laboratory jellyfish. *Curr Top Dev Biol*,
676 doi:10.1016/bs.ctdb.2021.12.014 (2022).
677 8 Lechable, M. *et al.* An improved whole life cycle culture protocol for the
678 hydrozoan genetic model Clytia hemisphaerica. *Biol Open* **9**,
679 doi:10.1242/bio.051268 (2020).
680 9 Momose, T. & Houliston, E. Two oppositely localised frizzled RNAs as axis
681 determinants in a cnidarian embryo. *PLoS Biol* **5**, e70,
682 doi:10.1371/journal.pbio.0050070 (2007).
683 10 Momose, T., Derelle, R. & Houliston, E. A maternally localised Wnt ligand
684 required for axial patterning in the cnidarian Clytia hemisphaerica. *Development*
685 **135**, 2105-2113, doi:10.1242/dev.021543 (2008).
686 11 Momose, T. *et al.* High doses of CRISPR/Cas9 ribonucleoprotein efficiently
687 induce gene knockout with low mosaicism in the hydrozoan Clytia hemisphaerica

688 through microhomology-mediated deletion. *Sci Rep* **8**, 11734,
689 doi:10.1038/s41598-018-30188-0 (2018).
690 12 Quiroga Artigas, G. *et al.* A gonad-expressed opsin mediates light-induced
691 spawning in the jellyfish Clytia. *Elife* **7**, doi:10.7554/eLife.29555 (2018).
692 13 Quiroga Artigas, G. *et al.* A G protein-coupled receptor mediates neuropeptide-
693 induced oocyte maturation in the jellyfish Clytia. *PLoS Biol* **18**, e3000614,
694 doi:10.1371/journal.pbio.3000614 (2020).
695 14 Lapebie, P. *et al.* Differential responses to Wnt and PCP disruption predict
696 expression and developmental function of conserved and novel genes in a
697 cnidarian. *PLoS Genet* **10**, e1004590, doi:10.1371/journal.pgen.1004590 (2014).
698 15 Condamine, T. *et al.* Molecular characterisation of a cellular conveyor belt in
699 Clytia medusae. *Dev Biol* **456**, 212-225, doi:10.1016/j.ydbio.2019.09.001 (2019).
700 16 Leclere, L. *et al.* The genome of the jellyfish Clytia hemisphaerica and the
701 evolution of the cnidarian life-cycle. *Nat Ecol Evol* **3**, 801-810,
702 doi:10.1038/s41559-019-0833-2 (2019).
703 17 Sinigaglia, C. *et al.* Pattern regulation in a regenerating jellyfish. *Elife* **9**,
704 doi:10.7554/eLife.54868 (2020).
705 18 Chari, T. *et al.* Whole-animal multiplexed single-cell RNA-seq reveals
706 transcriptional shifts across Clytia medusa cell types. *Sci Adv* **7**, eabh1683,
707 doi:10.1126/sciadv.abh1683 (2021).
708 19 Weissbourd, B. *et al.* A genetically tractable jellyfish model for systems and
709 evolutionary neuroscience. *Cell* **184**, 5854-5868 e5820,
710 doi:10.1016/j.cell.2021.10.021 (2021).
711 20 Leclere, L. *et al.* Maternally localized germ plasm mRNAs and germ cell/stem cell
712 formation in the cnidarian Clytia. *Dev Biol* **364**, 236-248,
713 doi:10.1016/j.ydbio.2012.01.018 (2012).
714 21 Fujita, S., Kuranaga, E. & Nakajima, Y. I. Regeneration Potential of Jellyfish:
715 Cellular Mechanisms and Molecular Insights. *Genes (Basel)* **12**,
716 doi:10.3390/genes12050758 (2021).
717 22 Fujiki, A., Hou, S., Nakamoto, A. & Kumano, G. Branching pattern and
718 morphogenesis of medusa tentacles in the jellyfish Cladonema pacificum

(Hydrozoa, Cnidaria). *Zoological Lett* **5**, 12, doi:10.1186/s40851-019-0124-4 (2019).

23 Fujita, S., Kuranaga, E. & Nakajima, Y. I. Cell proliferation controls body size growth, tentacle morphogenesis, and regeneration in hydrozoan jellyfish Cladonema pacificum. *PeerJ* **7**, e7579, doi:10.7717/peerj.7579 (2019).

24 Hou, S., Zhu, J., Shibata, S., Nakamoto, A. & Kumano, G. Repetitive accumulation of interstitial cells generates the branched structure of Cladonema medusa tentacles. *Development* **148**, doi:10.1242/dev.199544 (2021).

25 Takeda, N. *et al.* Identification of jellyfish neuropeptides that act directly as oocyte maturation-inducing hormones. *Development* **145**, doi:10.1242/dev.156786 (2018).

26 Stierwald, M., Yanze, N., Bamert, R. P., Kammermeier, L. & Schmid, V. The Sine oculis/Six class family of homeobox genes in jellyfish with and without eyes: development and eye regeneration. *Dev Biol* **274**, 70-81, doi:10.1016/j.ydbio.2004.06.018 (2004).

27 Suga, H., Schmid, V. & Gehring, W. J. Evolution and functional diversity of jellyfish opsins. *Curr Biol* **18**, 51-55, doi:10.1016/j.cub.2007.11.059 (2008).

28 Suga, H. *et al.* Flexibly deployed Pax genes in eye development at the early evolution of animals demonstrated by studies on a hydrozoan jellyfish. *Proc Natl Acad Sci U S A* **107**, 14263-14268, doi:10.1073/pnas.1008389107 (2010).

29 Graziussi, D. F., Suga, H., Schmid, V. & Gehring, W. J. The "eyes absent" (eya) gene in the eye-bearing hydrozoan jellyfish Cladonema radiatum: conservation of the retinal determination network. *J Exp Zool B Mol Dev Evol* **318**, 257-267, doi:10.1002/jez.b.22442 (2012).

30 Meister, G. & Tuschl, T. Mechanisms of gene silencing by double-stranded RNA. *Nature* **431**, 343-349, doi:10.1038/nature02873 (2004).

31 Rao, D. D., Vorhies, J. S., Senzer, N. & Nemunaitis, J. siRNA vs. shRNA: similarities and differences. *Adv Drug Deliv Rev* **61**, 746-759, doi:10.1016/j.addr.2009.04.004 (2009).

32 Moran, Y. *et al.* Cnidarian microRNAs frequently regulate targets by cleavage. *Genome Res* **24**, 651-663, doi:10.1101/gr.162503.113 (2014).

750 33 Watanabe, H. *et al.* Nodal signalling determines biradial asymmetry in Hydra.
751 *Nature* **515**, 112-115, doi:10.1038/nature13666 (2014).
752 34 Pankow, S. & Bamberger, C. The p53 tumor suppressor-like protein nvp63
753 mediates selective germ cell death in the sea anemone Nematostella vectensis.
754 *PLoS One* **2**, e782, doi:10.1371/journal.pone.0000782 (2007).
755 35 He, S. *et al.* An axial Hox code controls tissue segmentation and body patterning
756 in Nematostella vectensis. *Science* **361**, 1377-1380,
757 doi:10.1126/science.aar8384 (2018).
758 36 Karabulut, A., He, S., Chen, C. Y., McKinney, S. A. & Gibson, M. C.
759 Electroporation of short hairpin RNAs for rapid and efficient gene knockdown in
760 the starlet sea anemone, Nematostella vectensis. *Dev Biol* **448**, 7-15,
761 doi:10.1016/j.ydbio.2019.01.005 (2019).
762 37 DuBuc, T. Q. *et al.* Transcription factor AP2 controls cnidarian germ cell
763 induction. *Science* **367**, 757-762, doi:10.1126/science.aay6782 (2020).
764 38 Quiroga-Artigas, G., Duscher, A., Lundquist, K., Waletich, J. & Schnitzler, C. E.
765 Gene knockdown via electroporation of short hairpin RNAs in embryos of the
766 marine hydroid Hydractinia symbiolongicarpus. *Sci Rep* **10**, 12806,
767 doi:10.1038/s41598-020-69489-8 (2020).
768 39 Ha, M. & Kim, V. N. Regulation of microRNA biogenesis. *Nat Rev Mol Cell Biol*
769 **15**, 509-524, doi:10.1038/nrm3838 (2014).
770 40 Krishna, S. *et al.* Deep sequencing reveals unique small RNA repertoire that is
771 regulated during head regeneration in Hydra magnipapillata. *Nucleic Acids Res*
772 **41**, 599-616, doi:10.1093/nar/gks1020 (2013).
773 41 Moran, Y., Praher, D., Fredman, D. & Technau, U. The evolution of microRNA
774 pathway protein components in Cnidaria. *Mol Biol Evol* **30**, 2541-2552,
775 doi:10.1093/molbev/mst159 (2013).
776 42 Murchison, E. P., Partridge, J. F., Tam, O. H., Cheloufi, S. & Hannon, G. J.
777 Characterization of Dicer-deficient murine embryonic stem cells. *Proc Natl Acad*
778 *Sci U S A* **102**, 12135-12140, doi:10.1073/pnas.0505479102 (2005).
779 43 Kok, K. H., Ng, M. H., Ching, Y. P. & Jin, D. Y. Human TRBP and PACT directly
780 interact with each other and associate with dicer to facilitate the production of

781 small interfering RNA. *J Biol Chem* **282**, 17649-17657,
782 doi:10.1074/jbc.M611768200 (2007).
783 44 Watanabe, H. *et al.* Sequential actions of beta-catenin and Bmp pattern the oral
784 nerve net in Nematostella vectensis. *Nat Commun* **5**, 5536,
785 doi:10.1038/ncomms6536 (2014).
786 45 Schindelin, J. *et al.* Fiji: an open-source platform for biological-image analysis.
787 *Nat Methods* **9**, 676-682, doi:10.1038/nmeth.2019 (2012).
788 46 Fujita, S., Kuranaga, E., Miura, M. & Nakajima, Y. I. Fluorescent In Situ
789 Hybridization and 5-Ethynyl-2'-Deoxyuridine Labeling for Stem-like Cells in the
790 Hydrozoan Jellyfish Cladonema pacificum. *J Vis Exp*, doi:10.3791/64285 (2022).
791 47 Thompson, J. D., Higgins, D. G. & Gibson, T. J. CLUSTAL W: improving the
792 sensitivity of progressive multiple sequence alignment through sequence
793 weighting, position-specific gap penalties and weight matrix choice. *Nucleic Acids*
794 *Res* **22**, 4673-4680, doi:10.1093/nar/22.22.4673 (1994).
795 48 Waterhouse, A. M., Procter, J. B., Martin, D. M., Clamp, M. & Barton, G. J.
796 Jalview Version 2--a multiple sequence alignment editor and analysis workbench.
797 *Bioinformatics* **25**, 1189-1191, doi:10.1093/bioinformatics/btp033 (2009).
798 49 Kumar, S., Stecher, G., Li, M., Knyaz, C. & Tamura, K. MEGA X: Molecular
799 Evolutionary Genetics Analysis across Computing Platforms. *Mol Biol Evol* **35**,
800 1547-1549, doi:10.1093/molbev/msy096 (2018).
801 50 Deguchi, R., Kondoh, E. & Itoh, J. Spatiotemporal characteristics and
802 mechanisms of intracellular Ca(2+) increases at fertilization in eggs of jellyfish
803 (Phylum Cnidaria, Class Hydrozoa). *Dev Biol* **279**, 291-307,
804 doi:10.1016/j.ydbio.2004.11.036 (2005).
805 51 Scholz, C. B. & Technau, U. The ancestral role of Brachyury: expression of
806 NemBra1 in the basal cnidarian Nematostella vectensis (Anthozoa). *Dev Genes*
807 *Evol* **212**, 563-570, doi:10.1007/s00427-002-0272-x (2003).
808 52 Servetnick, M. D. *et al.* Cas9-mediated excision of Nematostella brachyury
809 disrupts endoderm development, pharynx formation and oral-aboral patterning.
810 *Development* **144**, 2951-2960, doi:10.1242/dev.145839 (2017).
811 53 Fourrage, C., Swann, K., Gonzalez Garcia, J. R., Campbell, A. K. & Houliston, E.
812 An endogenous green fluorescent protein-photoprotein pair in Clytia

813 hemisphaerica eggs shows co-targeting to mitochondria and efficient
814 bioluminescence energy transfer. *Open Biol* **4**, 130206, doi:10.1098/rsob.130206
815 (2014).
816 54 Guder, C. *et al.* The Wnt code: cnidarians signal the way. *Oncogene* **25**, 7450-
817 7460, doi:10.1038/sj.onc.1210052 (2006).
818 55 Lee, P. N., Pang, K., Matus, D. Q. & Martindale, M. Q. A WNT of things to come:
819 evolution of Wnt signaling and polarity in cnidarians. *Semin Cell Dev Biol* **17**,
820 157-167, doi:10.1016/j.semcdb.2006.05.002 (2006).
821 56 Kraus, Y., Aman, A., Technau, U. & Genikhovich, G. Pre-bilaterian origin of the
822 blastoporal axial organizer. *Nat Commun* **7**, 11694, doi:10.1038/ncomms11694
823 (2016).
824 57 Plickert, G., Jacoby, V., Frank, U., Muller, W. A. & Mokady, O. Wnt signaling in
825 hydroid development: formation of the primary body axis in embryogenesis and
826 its subsequent patterning. *Dev Biol* **298**, 368-378,
827 doi:10.1016/j.ydbio.2006.06.043 (2006).
828 58 Bartel, D. P. MicroRNAs: genomics, biogenesis, mechanism, and function. *Cell*
829 **116**, 281-297, doi:10.1016/s0092-8674(04)00045-5 (2004).
830 59 DuBuc, T. Q., Stephenson, T. B., Rock, A. Q. & Martindale, M. Q. Hox and Wnt
831 pattern the primary body axis of an anthozoan cnidarian before gastrulation. *Nat*
832 *Commun* **9**, 2007, doi:10.1038/s41467-018-04184-x (2018).
833 60 Yasuoka, Y., Shinzato, C. & Satoh, N. The Mesoderm-Forming Gene brachyury
834 Regulates Ectoderm-Endoderm Demarcation in the Coral Acropora digitifera.
835 *Curr Biol* **26**, 2885-2892, doi:10.1016/j.cub.2016.08.011 (2016).
836 61 Duffy, D. J., Plickert, G., Kuenzel, T., Tilmann, W. & Frank, U. Wnt signaling
837 promotes oral but suppresses aboral structures in Hydractinia metamorphosis
838 and regeneration. *Development* **137**, 3057-3066, doi:10.1242/dev.046631
839 (2010).
840 62 Krasovec, G., Pottin, K., Rosello, M., Queinnec, E. & Chambon, J. P. Apoptosis
841 and cell proliferation during metamorphosis of the planula larva of Clytia
842 hemisphaerica (Hydrozoa, Cnidaria). *Dev Dyn* **250**, 1739-1758,
843 doi:10.1002/dvdy.376 (2021).

63 Nath, R. D. *et al.* The Jellyfish Cassiopea Exhibits a Sleep-like State. *Curr Biol* **27**, 2984-2990 e2983, doi:10.1016/j.cub.2017.08.014 (2017).

64 Kanaya, H. J. *et al.* A sleep-like state in Hydra unravels conserved sleep mechanisms during the evolutionary development of the central nervous system. *Sci Adv* **6**, doi:10.1126/sciadv.abb9415 (2020).

65 Fuchs, B. *et al.* Regulation of polyp-to-jellyfish transition in Aurelia aurita. *Curr Biol* **24**, 263-273, doi:10.1016/j.cub.2013.12.003 (2014).

66 Lommel, M. *et al.* Hydra Mesoglea Proteome Identifies Thrombospondin as a Conserved Component Active in Head Organizer Restriction. *Sci Rep* **8**, 11753, doi:10.1038/s41598-018-30035-2 (2018).

Acknowledgement

We thank R. Deguchi (Miyagi Univ. Education, Japan) for sharing *Cladonema pacificum* and EMBRC France for sharing *Clytia hemisphaerica*. We thank T. Momose (Sorbonne University, CNRS, France) for helpful discussion. We thank I. Nagai, H. Nakatani, and A. Sasaki for technical assistance; and A. Dahal, A. Tanimoto, and J. Higuchi for *Nematostella* culture. This work was supported by JST grant number JPMJCR1852 to E.K., AMED under grant number JP21gm6110025 to Y.N., and the JSPS KAKENHI grant numbers JP21H05255 to E.K., and JP17H06332, JP19K22550, JP22H02762 to Y.N.

Author contributions

T.M.-O. conceptualized and designed the project, performed experiments using jellyfish, analyzed data, prepared figures, and wrote the manuscript. S.F. performed experiments and analyzed data. R.N. performed experiments using *Nematostella*. H.W. conceptualized and designed the project. E.K. contributed reagents. Y.N. conceptualized and designed the project, prepared figures, and wrote the manuscript. All authors approved the final manuscript.

Data availability

The datasets used and/or analysed during the current study are available from the corresponding author on reasonable request and nucleotide sequences are available in the GenBank/EMBL/DDBJ under the accession numbers (*CpWnt1*, LC720432; *CpWnt1b*, LC720433; *CpWnt2*, LC720434; *CpWnt3*, LC720435; *CpWnt5*, LC720436; *CpWnt6*, LC720437; *CpWnt8*, LC720438; *CpWntA*, LC720439; *CpBrachyury*, LC720440; *CpFoxQ2a*, LC720441; *F-actin capping protein subunit beta*, LC720442; *CpEF1alpha*, LC720443).

Competing interests

The authors declare no competing interests.

Figure legends

Figure 1. The hydrozoan jellyfish *Clytia hemisphaerica* and *Cladonema pacificum*. (**A**) Cladogram depicting the phylogenetic position of cnidarian jellyfish. As the sister group of Bilateria, the phylum Cnidaria is divided into two clades, Anthozoa and Medusozoa, which consists of four classes: Hydrozoa, Staurozoa, Scyphozoa, and Cubozoa. Hydrozoa includes polyp type animals without a medusa stage (e.g. *Hydra* and *Hydractinia*) and jellyfish that have both polyp and medusa stages (e.g. *Clytia* and *Cladonema*). (**B** and **C**) Photos of an adult medusa and the eggs of *Clytia hemisphaerica* (**B**) and *Cladonema pacificum* (**C**). Scale bars: 1 mm for medusae; 100 μm for eggs.

Figure 2. The electroporation procedure for jellyfish eggs. (**A**) Schematic of spawning under the 24 h light/dark cycle. *Clytia hemisphaerica* are maintained on a 13 h dark/11 h light cycle. After light stimuli, sperm spawning occurs within 60-90 min and egg spawning occurs within 90-120 min. *Cladonema pacificum* are maintained on a 23.5 h light/0.5 h dark cycle. After dark stimuli, sperm and egg spawning occurs within

908 25 min. (**B**) Fertilized eggs are resuspended in 15% Ficoll/artificial sea water to prevent
909 precipitation of eggs during electroporation. (**C**) Electroporation is performed with the
910 Bio-Rad Gene Pulser Xcell electroporation system and a cuvette with a 4 mm gap. (**D**)
911 Visualization of the Rhodamine-Dextran delivery into eggs by electroporation.
912 Rhodamine is shown in red. While little or no fluorescence was observed in eggs
913 without electroporation (No EP), under the condition of a single 50 V pulse for 25 ms,
914 rhodamine signals were detected in both *Clytia and Cladonema* eggs without cell
915 damage. For clarity, egg outlines are indicated with dashed lines for eggs without
916 electroporation. Scale bars: 200 μm.
917
918
919 **Figure 3**. **Phenotypes of *GFP1* knockdown with siRNA in *Clytia* fertilized eggs.** (**A**)
920 Schematic of the siRNA electroporation procedure using fertilized eggs. Fertilized eggs
921 in 15% Ficoll/artificial sea water mixed with siRNA are incubated for 5 min, and
922 electroporation is conducted after transferring into a cuvette. (**B** and **C**) Phenotypes of
923 *Clytia* 2-day planula after *CheGFP1* siRNA knockdown. (**D**) Boxplots showing the GFP
924 fluorescence intensity mean values in 2-day planula after electroporation of 0 and 600
925 ng/μl siRNAs targeting *CheGFP1*. Center lines indicate the medians; x's denote the
926 means; box limits represent the 25th and 75th percentiles; whiskers show the maximum
927 and minimum values. 0 ng/μl, n=24; 600 ng/μl, n=81. ***p<0.001. (**E**-**H**) Phenotypes of
928 3-day planula after siRNA targeting *CheGFP1* electroporation (0, 150, 300, and 600
929 ng/μl si*CheGFP1*). (**I** and **J**) For quantification of green fluorescence, we classified
930 phenotypes into two categories: planula with ring-like green fluorescence as "wild-type,"
931 and planula with reduced green fluorescence as "reduced". (**K**) Quantification of planula
932 larvae positive for *CheGFP1* (wild-type). Bar plots show the percentage of wild-type
933 phenotype after *CheGFP1* knockdown. Number of examined planula: 0 ng/μl, *n*=82; 150
934 ng/μl, *n*=64; 300 ng/μl, *n*=58; 600 ng/μl, *n*=114. Error bars: maximum and minimum
935 values. Experiments were repeated three times. p-values: 150 ng/μl, p=0.064505; 300
936 ng/μl, p=0.001437; 600 ng/μl, p=0.00066. **p<0.01, ***p<0.001. (**L**) Quantification of
937 *CheGFP1* mRNA expression levels in 3-day planula by RT-qPCR. *CheEF1alpha* was
938 used as an internal control. Bar heights represent mean values of at least three
939 independent experiments. *CheGFP1* expression levels are standardized relative to the

940 control (0 ng/μl) condition. Error bars: standard deviation. Experiments were performed
941 in triplicated and repeated at least three times. p-values: 150 ng/μl, p=0.829361; 300
942 ng/μl, p=0.08588; 600 ng/μl, p=0.037359. *p<0.05. Scale bars: 200 μm.
943
944
945 **Figure 4. Phenotypes of *Wnt3* knockdown with siRNA in *Clytia* fertilized eggs.** (**A**
946 and **B**) Typical phenotypes of *Clytia* 1-day planula. While morphologies of control
947 planula (0 ng/μl) have an elongated oval-shape (A), those of *CheWnt3* siRNA (400
948 ng/μl) are spherical in shape (**B**). (**C**) Schematic of ellipse approximation for planula
949 morphology and calculation of the aspect ratio. The aspect ratio was calculated by
950 dividing the long axis (a) by short axis (b). (**D**) Boxplots showing the aspect ratio of the
951 1-day planula. Center lines show the medians; x's denote the mean values; box limits
952 indicate the 25th and 75th percentiles; whiskers show maximum and minimum values;
953 inner points and outliers are represented by circles. Number of examined planula: 0
954 ng/μl, *n*=127; 400 ng/μl. *n*=25, ***p<0.001. (**E**-**H**) Phenotypes of 1-day planula after
955 siRNA targeting *CheWnt3* electroporation (0, 100, 200, and 400 ng/μl si*CheWnt3*). (**I**
956 and **J**) For morphology quantification, we classified planula phenotypes into two
957 categories: elongated oval shape as "normal" and spherical (circle) shape as
958 "spherical". (**K**) Bar plots show the percentage of normal phenotypes across four
959 different siRNA doses as well as planulae treated with shRNA and siNC, a siRNA
960 universal negative control. Percentages are the mean value and error bars indicate
961 standard deviation. Numbers of examined planula: 0 ng/μl, *n*=127; 100 ng/μl, *n*=75; 200
962 ng/μl, *n*=86; 400 ng/μl, *n*=95. shRNA 400 ng/μl, *n*=288; siNC 400 ng/μl, *n*=45.
963 Experiments were repeated three times. Error bars: maximum and minimum values. p-
964 values: 100 ng/μl, p=0.000599; 200 ng/μl, p=0.000438; 400 ng/μl, p=0.000402; 400
965 ng/μl of shRNA, p=0.031928; 400 ng/μl of siNC, p=0.283359. *p<0.05, ***p<0.001. (**L**)
966 Quantification of *CheWnt3* mRNA levels of 1-day planula by RT-qPCR. *CheEF1alpha*
967 was used as an internal control. Bar heights represent the mean value. *CheWnt3*
968 expression levels are standardized relative to the control (0 ng/μl). Error bars: standard
969 deviation. p-values: 100 ng/μl, p= 0.00799; 200 ng/μl, p= 0.000754; 400 ng/μl, p=
970 0.000733; 400 ng/μl of shRNA, p= 0.095403; 400 ng/μl of siNC, p= 0.900264. **p<0.01,

971 ***p<0.001. n.s., not significant. Experiments were performed in triplicate and repeated
972 at least three times. Scale bars: (A, B, E-H) 400 μm, (I, J) 100 μm.
973
974
975 **Figure 5. Phenotypes of *Wnt3* knockdown with siRNA in *Cladonema* fertilized**
976 **eggs.** (**A**) Typical morphology of *Cladonema* egg and planula. The wild-type
977 *Cladonema* planula larvae exhibit a slight oval shape. To deliver siRNAs targeting
978 *CpWnt3,* electroporation was performed in fertilized eggs (1-cell stage), and phenotypes
979 were confirmed at planula in one day. (**B** and **C**) Phenotypes of 1-day planula after
980 *CpWnt3* siRNA knockdown. (**D**) Schematic of ellipse approximation for planula
981 morphology and calculation of the aspect ratio. The aspect ratio was calculated by
982 dividing the long axis (a) by short axis (b). (**E**) Boxplots showing the aspect ratio of the
983 1-day planula after si*CpWnt3* electroporation (0 and 300 ng/μl). Center lines show the
984 medians; x's denote the mean values; box limits indicate the 25th and 75th percentiles;
985 whiskers show maximum and minimum values; inner points and outliers are
986 represented by circles. Number of examined planulae: 0 ng/μl, *n*=22; 300 ng/μl, *n*=50.
987 p= 0.658303. n.s., not significant. (**F**) Quantification of *CpWnt3* mRNA levels in 1-day
988 planula by RT-qPCR. *CpEF1alpha* was used as an internal control. Bar heights
989 represent the mean value. Error bars indicate standard deviation. *CpWnt3* expression
990 levels are standardized relative to the control (0 ng/μl). Experiments were performed in
991 triplicate and repeated three times. p-values: 150 ng/μl, p= 0.376498; 300 ng/μl, p=
992 0.073956. (**G, H**) Representative *in situ* hybridization (ISH) image of oral *CpBra*
993 expression in 1-day planula for control (G: 0 ng/μl si*CpWnt3*) and *CpWnt3* siRNA (H:
994 300 ng/μl si*CpWnt3*). The oral pole is indicated by an asterisk. (**I**) Quantification of
995 *CpBra* expression phenotypes based on ISH images. Stacked bar plots show the
996 percentage of 1-day planulae in each phenotypic class. *CpBra* expression patterns are
997 categorized into three phenotypes (strong, weak and none). 0 ng/μl, *n*=74; 300 ng/μl,
998 *n*=58. Scale bars: (B, C) 200 μm, (G, H) 50 μm.

Figure 1

Masuda-Ozawa et al.

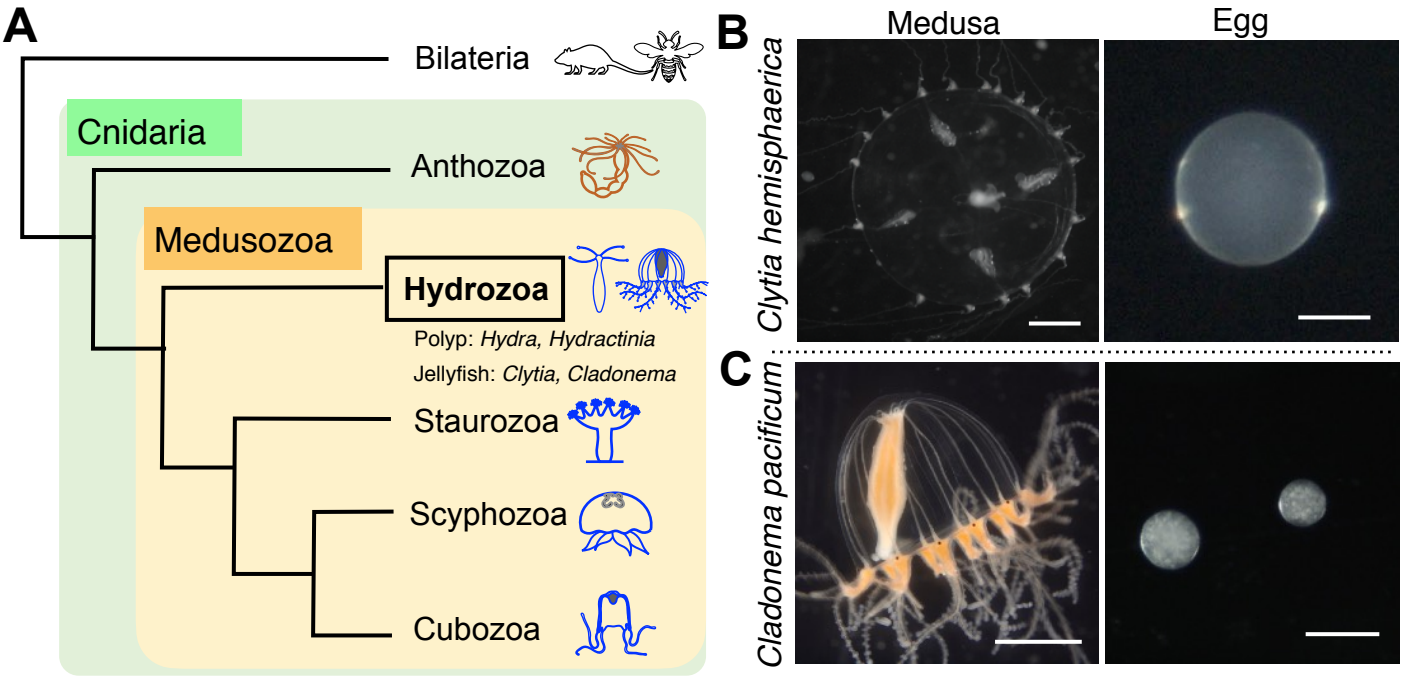

Figure 2

Masuda-Ozawa et al.

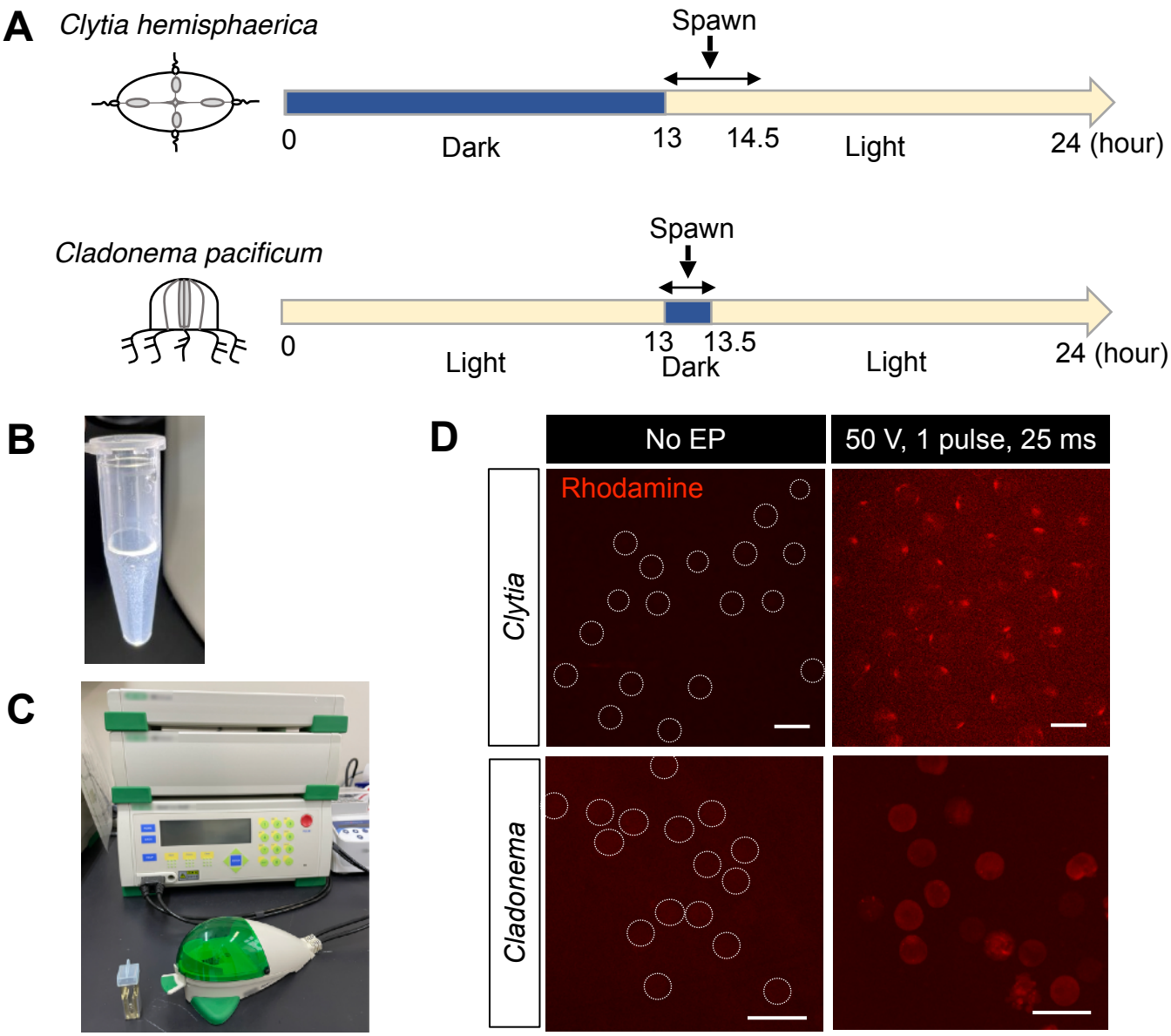

Figure 3

Masuda-Ozawa et al.

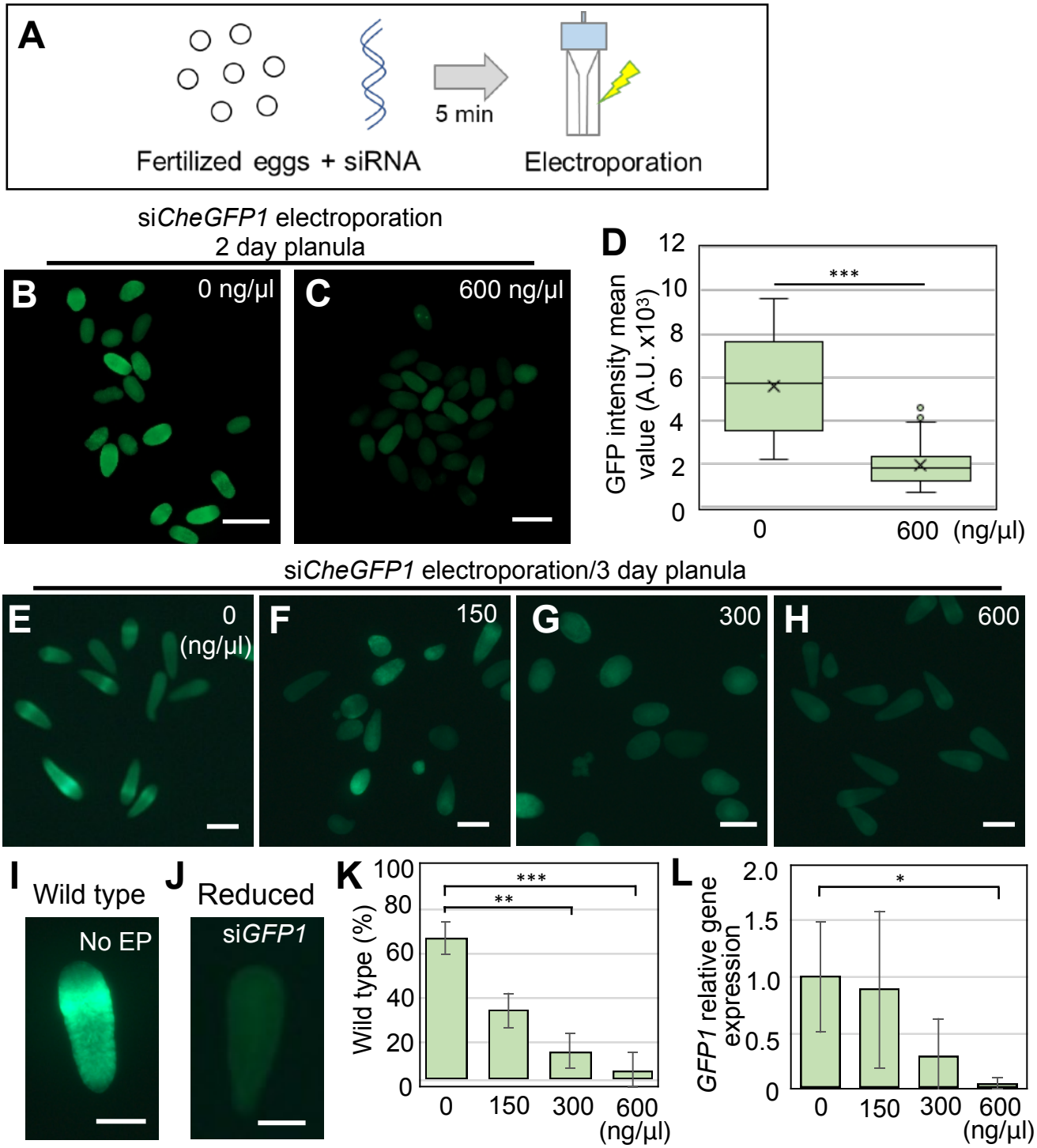

Figure 4

Masuda-Ozawa et al.

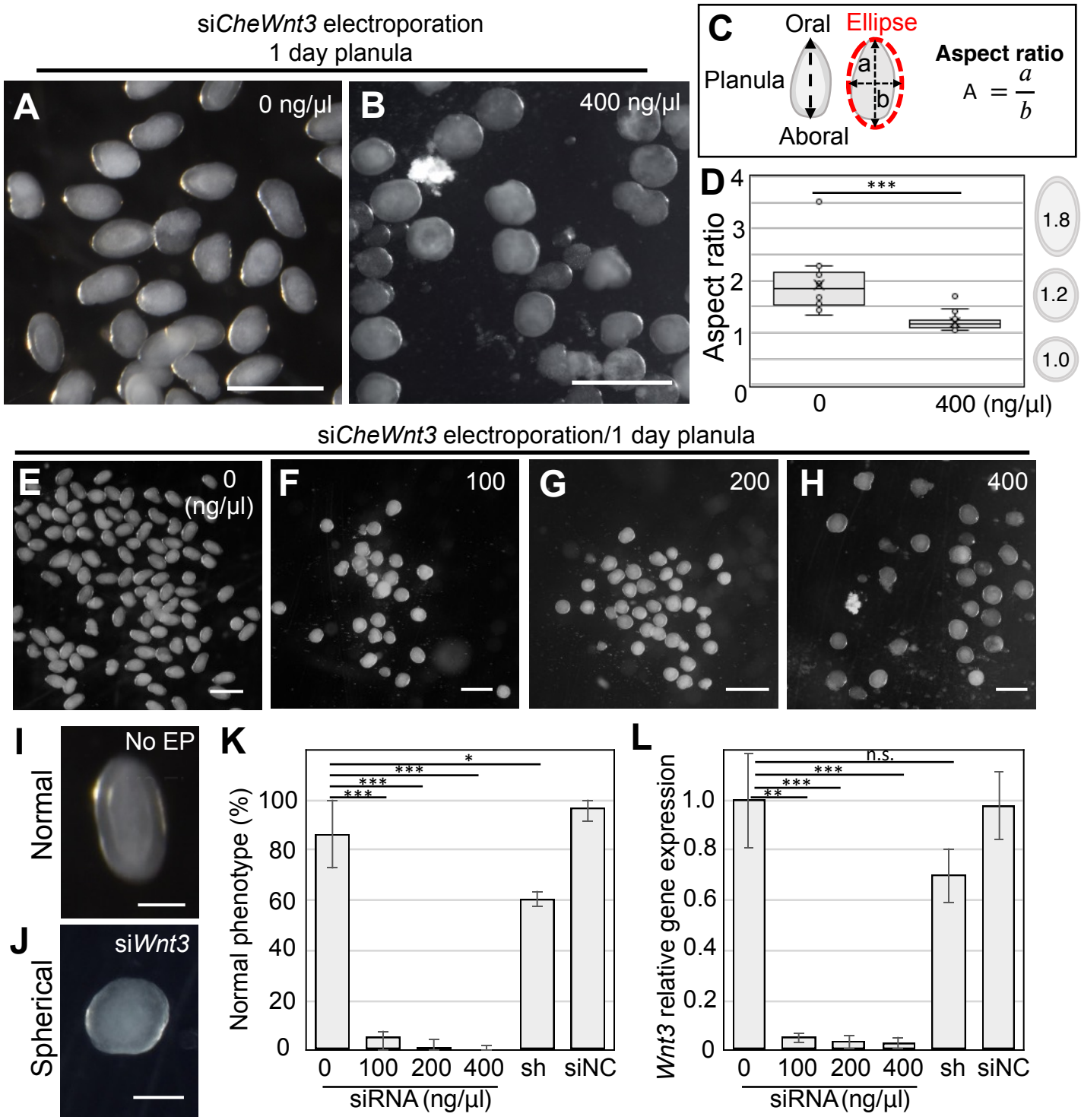

Figure 5
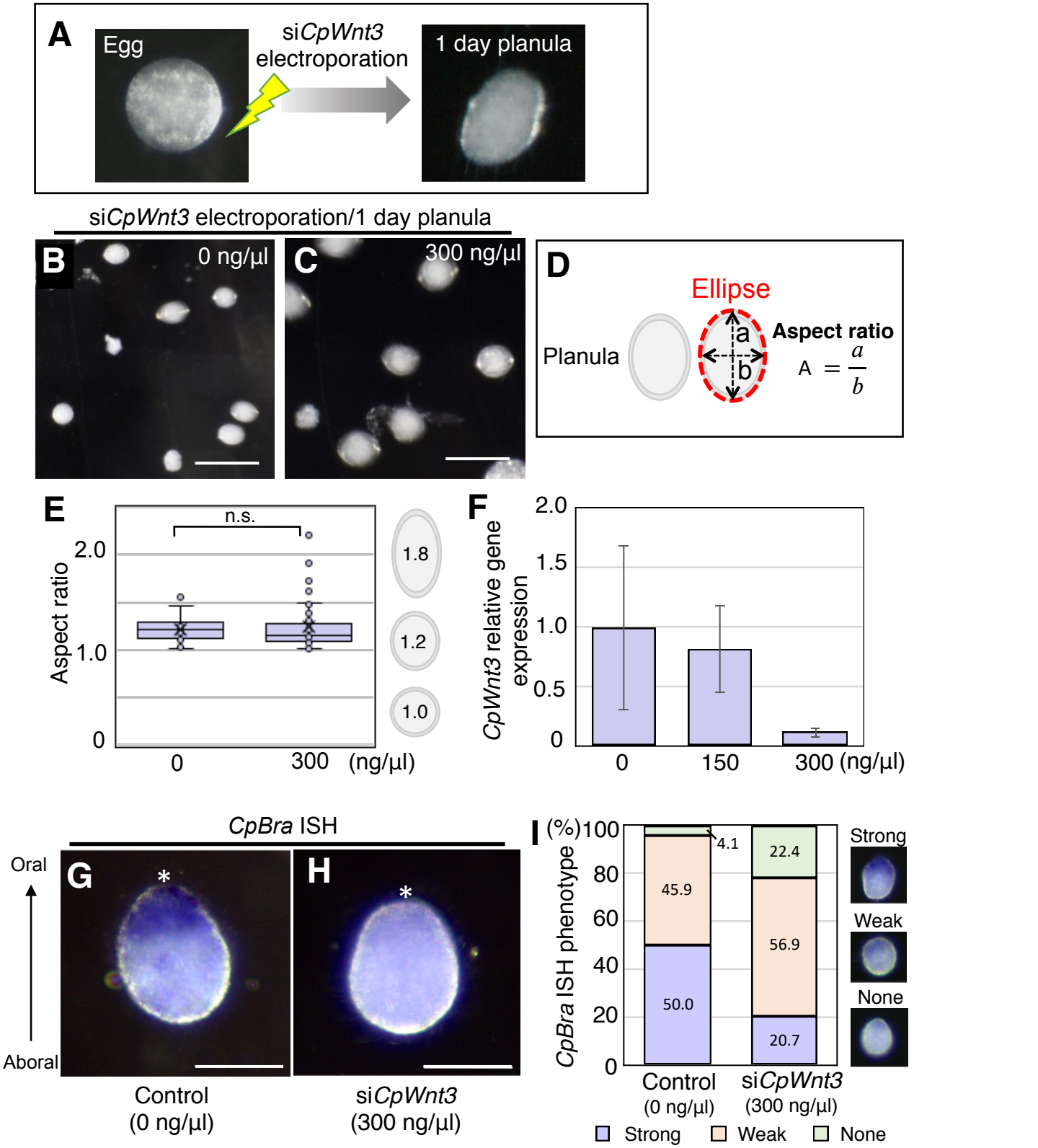
Masuda-Ozawa et al.